Structural aspects of the 530 °C phase transition in $LaBGeO_5$



1997 J. Phys.: Condens. Matter 9 3503

(http://iopscience.iop.org/0953-8984/9/17/002)

J. Phys.: Condens. Matter **9** (1997) 3503–3519. Printed in the UK PII: S0953-8984(97)81230-1

# Structural aspects of the 530 °C phase transition in $LaBGeO_5$

E L Belokoneva†, W I F David, J B Forsyth and K S Knight
Rutherford Appleton Laboratory, Chilton, Oxon OX11 0QX, UK

Received 23 January 1997, in final form 12 February 1997

**Abstract.** High-resolution neutron powder diffractometry has been used to characterize the structural phase transition which occurs in $LaBGeO_5$ at 530 °C. The change in lattice parameters of the trigonal unit cell as a function of temperature, observed in the range from ambient to 700 °C, shows that the transition from the polar space group $P3_1$ to the non-polar space group $P3_121$ is associated with a collapse of the $a$-dimension, whereas the $c$-dimension and the cell volume increase monotonically with small changes of slope at the transition temperature. The structure of the lower-temperature phase, previously determined at ambient temperature by single-crystal x-ray diffraction, has been refined at 20, 500 and 525 °C and the structure of the higher-temperature phase determined from data taken at 535, 560 and 630 °C.

The thermal evolution of the atomic coordinates shows that the deciding role in the transition is provided by a complex movement of the B–O tetrahedron, in which the main component is a rotation around the $3_1$ axis. The transition is continuous and results from structural changes which are displacive but also show order–disorder character. This conclusion is in accordance with the known thermal, optical and dielectric properties of this new multifunction (laser, ferroelectric and non-linear optic) material. In the high-temperature modification, the dynamically disordered double helical chain of B–O tetrahedra has no polarity in the $c$-direction. This is the main structural reason for the absence of ferroelectric properties above 530 °C.

The lower transition temperature of 140 °C in the related phase $LaBSiO_5$ may be understood by comparing the structural aspects of its transition with those of $LaBGeO_5$ using the Abrahams–Jamieson–Kurtz criteria. The effect of isomorphic substitution for Ge with the smaller Si atoms is equivalent to pressure being applied to the helical B chain and results in a chain which is more tilted in the silicate than in the germanate.

## 1. Introduction

Silicates and germanates form a vast array of inorganic structure types. Many of these possess acentric or polar space groups and are promising candidates for technical applications. In this paper we discuss materials that possess the crystal structure of the natural borosilicate stillwellite $CeBSiO_5$ [1] which is acentric, polar and belongs to space group $P3_1$. $RBGeO_5$ crystals were synthesized with R = (La, . . . , Er, Y). The lighter rare-earth compounds from La to Pr possess the stillwellite structure, determined in an x-ray single-crystal diffraction study of $LaBGeO_5$ [2]. The [001] projection of the structure is illustrated in figure 1; the trigonal unit-cell dimensions are $a = 7.020(5), c = 6.879(4)$ Å, space group $P3_1$ with $Z = 3$.

In contrast, the heavier rare earths Nd to Er and Y form crystals that are isostructural with another borosilicate mineral, datolite $CaBSiO_4(OH)$, which is centrosymmetric, $P2_1/a$. A

† Permanent address: Geological Faculty, Moscow State University, 119899 Moscow, Russia.

0953-8984/97/173503+17$19.50  

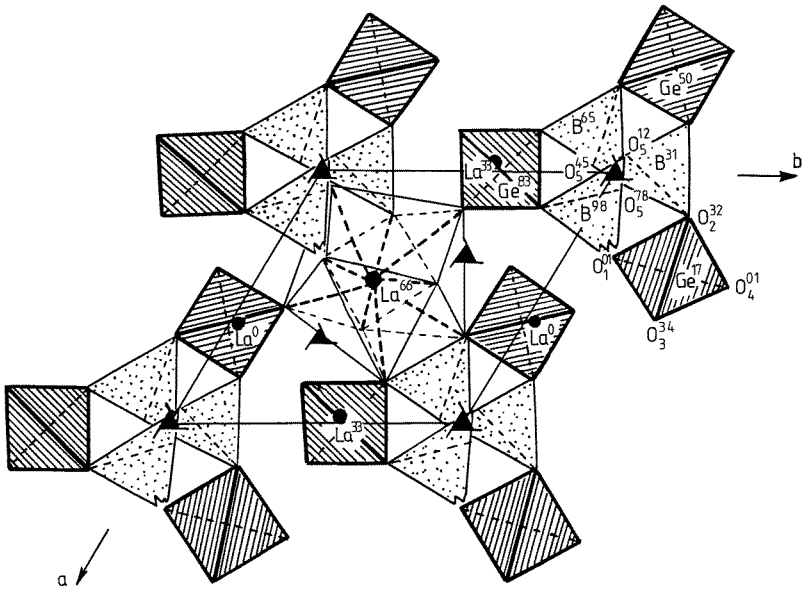


**Figure 1.** The [001] projection of the polar stillwellite structure of $LaBGeO_5$ at ambient temperature [2]. Some of the cation and oxygen positions are numbered with their percentage heights in the unit cell.

single-crystal x-ray structure refinement has been performed on $NdBGeO_5$ [2]. The change in structure type is principally connected with the change in ionic radii of the rare-earth ions, since the decrease in radius which occurs with increasing atomic number leads to a change in coordination of the rare-earth ion from nine in the stillwellite to eight in the datolite structure. The change in structure type occurs at Nd and this is typical of the rare-earth dependence of many silicate and germanate structures. In the series $RBGeO_5$, both Nd and its heavier neighbour Sm exhibit both structure types, with the higher-temperature phase being centrosymmetric and isomorphous with datolite.

The laser properties of $LaBGeO_5$ have been investigated using large crystals of optical quality grown by the Czochralski method [3]. The ability to produce such crystals containing a sufficiently high concentration of $Nd^{3+}$ ions in the La site makes this new material more favourable as an effective self-doubling laser than other candidates such as $LiNbO_3$ and $YAl_3(BO_3)_4$. Previous room temperature studies of $LaBGeO_5$ include its stimulated emission [3] and its Raman, second-harmonic generation, absorption and luminescence spectra [4–6]. It should also be noted that $LaBGeO_5$ is a good piezoelectric.

Measurements of the dielectric constants on a single crystal and of the intensity of second-harmonic generation of a powdered specimen of $LaBGeO_5$ as a function of temperature [7] were the first to show that this compound has two anomalies at 515 and 520 °C which the authors associated with first- and second-order phase transitions, respectively. Recently, however, both the temperature dependence of the dielectric constants and the dielectric loss [8] and of the specific heat [9] have been measured on single-crystal material, the former detecting a single transition at 531.5(1) °C and the latter a single transition at 529.5 °C. Both sets of authors conclude that the transition is close to, if not exactly, second order in character. Stefanovich *et al* [7] and Onodera *et al* [9] comment that, although the Landau coefficients indicate an order–disorder mechanism, the relatively

small entropy change associated with the transition is typical of a phase change which is displacive in character. This uncertainty about the structural basis for the transition has led us to study the thermal evolution of the structural parameters of the low-temperature phase as well as to determine the structure of the high-temperature phase.

We now report a high-resolution neutron powder study of $LaBGeO_5$. The temperature dependence of the unit-cell dimensions from 275 to 700 °C has been determined from some forty short runs and clearly confirms that the phase transition at 530(1) °C is continuous and of second order. In addition, these data have enabled us to follow the movement of the atom positions throughout the temperature range and provide insight into the mechanism which drives the transition. Longer runs at 20, 500 and 525 °C, below the transition, and at 535, 560 and 630 °C, above the transition, have been used to refine, respectively, more accurate parameters for the lower-temperature stillwellite structure as the transition is approached and to determine the structure of the higher-temperature phase.

## 2. Experimental details

The powder specimen of $LaBGeO_5$ was prepared by crushing and grinding single-crystal material prepared using the Czochralski method [3]. Some 16 g of the powder with particle size less than 150 $\mu$m were sealed in a thin-walled vanadium sample can of rectangular cross section $40 \times 23 \times 3$ mm and oriented in a furnace on the HRPD high-resolution diffractometer at the ISIS pulsed neutron facility so that the minor dimension of the can was parallel to the incident neutron beam and the major dimension was vertical. This geometry was chosen to optimize the diffracted intensity into the backward-angle bank of detectors from an absorbing specimen. However, subsequent measurements of the wavelength dependence of the sample absorption showed that the boron was almost entirely composed of the non-absorbing $^{11}$B isotope. Vanadium was also used as the material for the furnace windows and resistance heating elements to reduce their contribution to the features of the diffraction patterns at the expense of an increase in the incoherent background. Time-of-flight data were collected in the range 30–130 ms at a 10 Hz repetition rate, normalized using the spectra from the main beam monitor and corrected for the wavelength dependence of the detector and the specimen absorption. The data sets used in the Rietveld refinements extended from 35–115 ms, corresponding to a range of $d$-spacing between 0.7 and 2.3 Å. Short runs of approximately 30 minutes' duration (total incident proton beam current 15 $\mu$A h) provided patterns which could be refined to give unit-cell dimensions precise to parts in $10^5$ and were also used to follow the temperature dependence of the structural parameters. Longer runs for accurate structure refinements at 500, 525, 535, 560 and 630 °C were each accumulated for 300 $\mu$A h, together with a 40 $\mu$A h run at ambient (20 °C). Structural analysis was performed using the Rietveld method using programs based on the Cambridge Crystallographic Subroutine Library (CCSL).

## 3. The temperature variation of the unit-cell dimensions from ambient to 700 °C

Figure 2 illustrates the behaviour of the unit-cell dimensions and the cell volume of $LaBGeO_5$ as a function of temperature. The $c$-dimension increases by 0.062 Å from 6.887 to 6.949 Å, whereas the $a$-axis decreases by 0.010 Å from 7.002 to 6.992 Å in the same temperature interval; the $a/c$ ratio changes from 1.0206 at room temperature through 1.0097 (525 °C) and 1.0088 (535 °C) to 1.0073 at 630 °C (table 1). The temperature at which the phase transition occurs (530 °C) is well determined from figures 2(a) and 2(b) in which

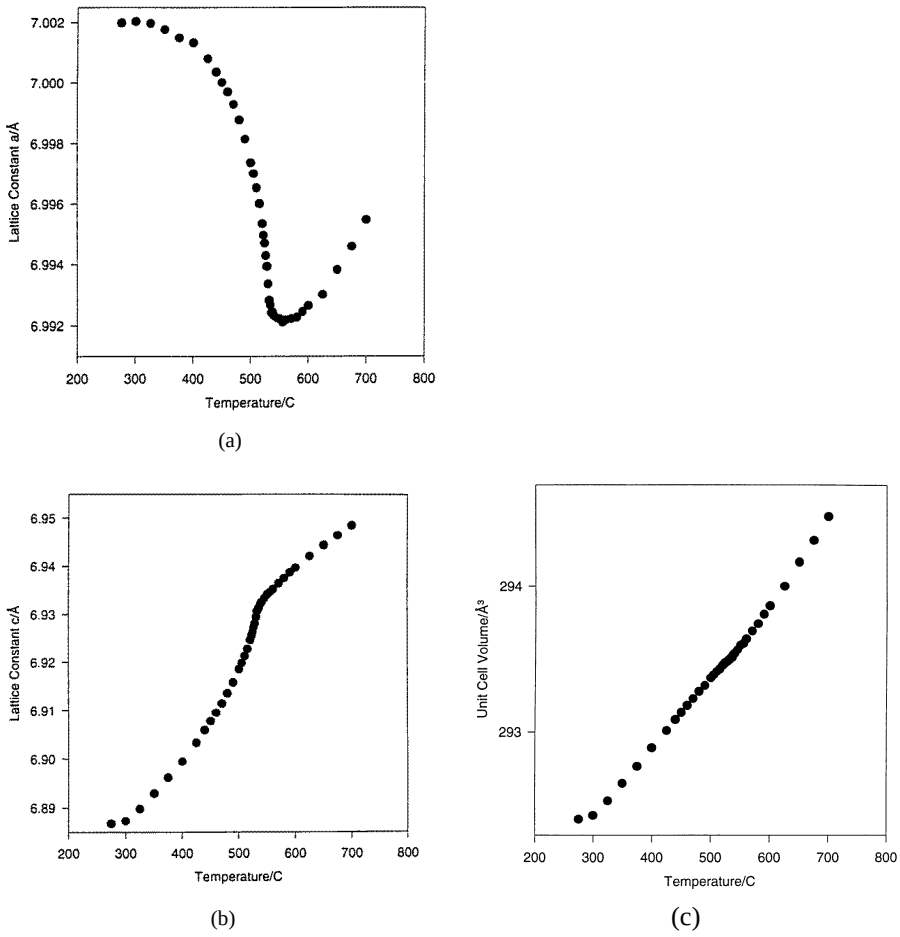


**Figure 2.** The temperature variation of the trigonal unit-cell dimensions of $LaBGeO_5$: (a) $a$, (b) $c$, and (c) the volume. The estimated standard deviations are smaller than the plotting symbol.

the curves change slope or have a cusp, respectively. In a recent investigation of the phase transition in the isomorphous phase $LaBSiO_5$, $T_c = 140\ ^\circ$C [10], the $a/c$ ratio was found to change from 1.0096 at room temperature to 1.0071 at 200 °C, which suggests that the $a/c$ ratio is a sensitive characteristic of the phase transition in the stillwellite structure type. The unit-cell volume of $LaBGeO_5$ increases monotonically with increasing temperature (figure 2(c)), which provides conclusive evidence that the phase transition is continuous and of second order.

## 4. The thermal evolution of the structure of the low-temperature phase of $LaBGeO_5$

As can be seen from figure 1, the coordination of oxygen about B, Ge and La in the stillwellite structure of $LaBGeO_5$ is fourfold, fourfold and ninefold, respectively. The structure is highly pseudosymmetric resulting from small atomic displacements (especially of O5 and B) from a structure which may be described within the acentric, but non-polar space group $P3_121$ but not within $P3_112$ [1, 2]; accordingly it has been suggested [5] that

**Table 1.** The temperature variation of the lattice parameters $a$ and $c$ of trigonal $LaBGeO_5$. The estimated standard deviations are (1) and (2) in the least-significant figures quoted, respectively.

| $T$ (°C) | $a$ (Å) | $c$ (Å) | $T$ (°C) | $a$ (Å) | $c$ (Å) |
|---|---|---|---|---|---|
| 20 | 7.0018 | 6.8606 | 526 | 6.9943 | 6.9273 |
| 275 | 7.0020 | 6.8868 | 528 | 6.9939 | 6.9281 |
| 300 | 7.0020 | 6.8873 | 530 | 6.9934 | 6.9294 |
| 325 | 7.0020 | 6.8897 | 532 | 6.9928 | 6.9306 |
| 350 | 7.0018 | 6.8930 | 534 | 6.9927 | 6.9312 |
| 375 | 7.0015 | 6.8962 | 536 | 6.9924 | 6.9317 |
| 400 | 7.0013 | 6.8995 | 538 | 6.9925 | 6.9321 |
| 425 | 7.0008 | 6.9033 | 540 | 6.9923 | 6.9325 |
| 440 | 7.0004 | 6.9059 | 545 | 6.9923 | 6.9333 |
| 450 | 7.0000 | 6.9077 | 550 | 6.9922 | 6.9341 |
| 460 | 6.9997 | 6.9095 | 555 | 6.9921 | 6.9346 |
| 470 | 6.9993 | 6.9114 | 560 | 6.9922 | 6.9352 |
| 480 | 6.9988 | 6.9135 | 570 | 6.9922 | 6.9364 |
| 490 | 6.9981 | 6.9158 | 580 | 6.9923 | 6.9375 |
| 500 | 6.9974 | 6.9186 | 590 | 6.9925 | 6.9387 |
| 505 | 6.9970 | 6.9199 | 600 | 6.9927 | 6.9396 |
| 510 | 6.9965 | 6.9213 | 625 | 6.9930 | 6.9421 |
| 515 | 6.9960 | 6.9228 | 630 | 6.9932 | 6.9427 |
| 520 | 6.9953 | 6.9246 | 650 | 6.9938 | 6.9444 |
| 522 | 6.9950 | 6.9256 | 675 | 6.9946 | 6.9464 |
| 524 | 6.9947 | 6.9263 | 700 | 6.9955 | 6.9485 |

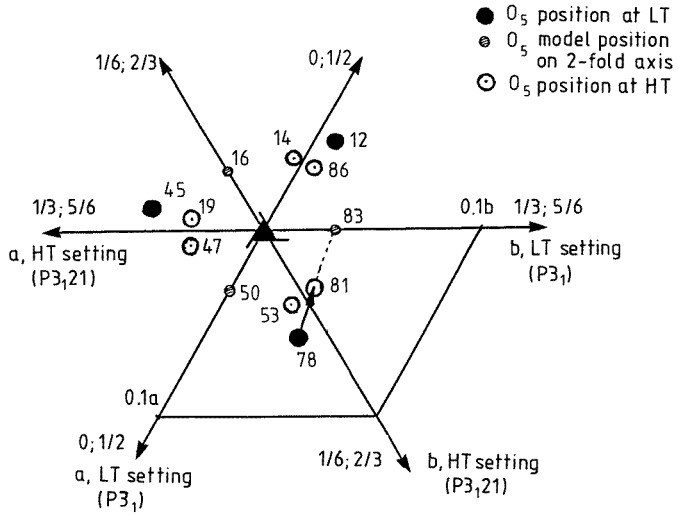


**Figure 3.** The positions of O5 in $LaBGeO_5$ in the model LT and HT modifications; the twofold axes are shown and the arrow indicates the displacement of O5.

this can be the structural basis for the phase transition at 530 °C. Our first model for the high-temperature phase followed this suggestion. The cations La, Ge and B are all located on a horizontal twofold axis (special position of symmetry 2); the positions of the O1, O2 and the O3, O4 pairs of oxygen anions are now connected by the same twofold axis to form two independent oxygen ions instead of the four in the low-temperature phase. The

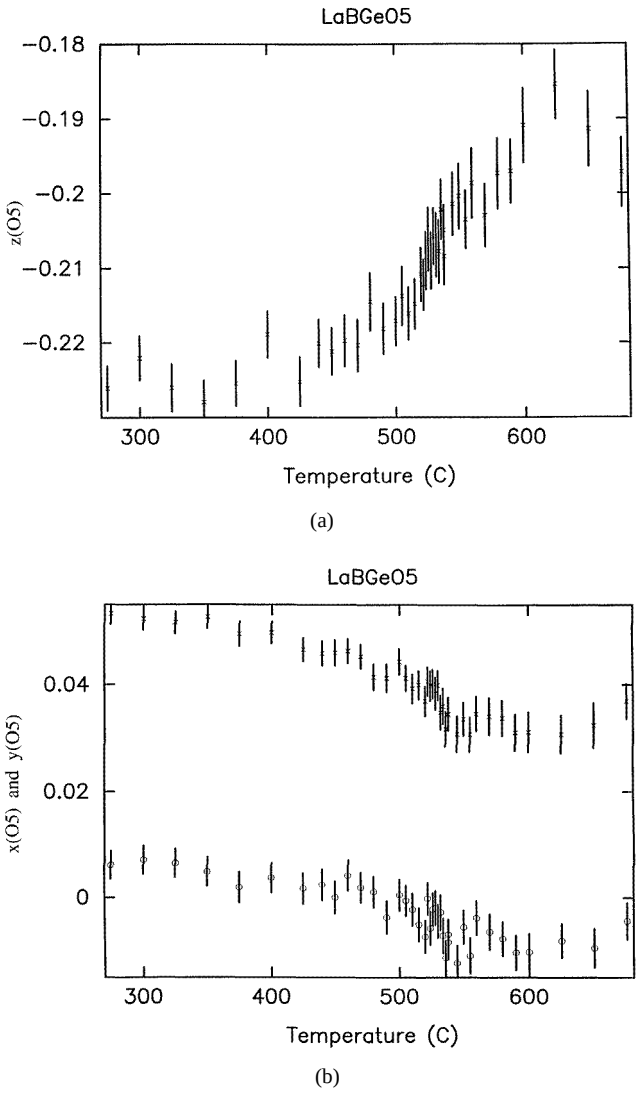


**Figure 4.** The thermal evolution of the atomic coordinates (a) $z$(O5); (b) $x$(O5) and $y$(O5); (c) $z$(O1) and $z$(O2); (d) $y$(O1) and $x$(O2); (e) $x$(O3) and $y$(O4); (f) $z$(O3) and $-z$(O4); (g) $z$(B). In figures (b) to (f), the first-mentioned parameter is plotted as open circles and the second as crosses.

remaining O5 ion, which has a roughly diagonal position [2] ($x \sim 0.0567$, $y \sim 0.0436$) between $a$ and $b$ in the low-temperature phase (figure 3) must either move ~0.48 Å to the nearest twofold axis parallel to $b$ at $z \cong 5/6$ or, alternatively, move through roughly double the distance, ~0.82 Å, to reach another twofold diagonal axis at $z \cong 2/3$. The necessary displacements are small for La and Ge and a little larger for O1, O2, O3 and O4. The biggest change occurs with the O5 position, not solely from the point of view of its displacement, but more from the necessarily large rotation—part of a complex movement of the B–O coordination tetrahedron—in which the O5 position (and appropriate O5–O5′ edge) rotates ~60° around the $3_1$ axis (figure 3). However, refinements of this model using

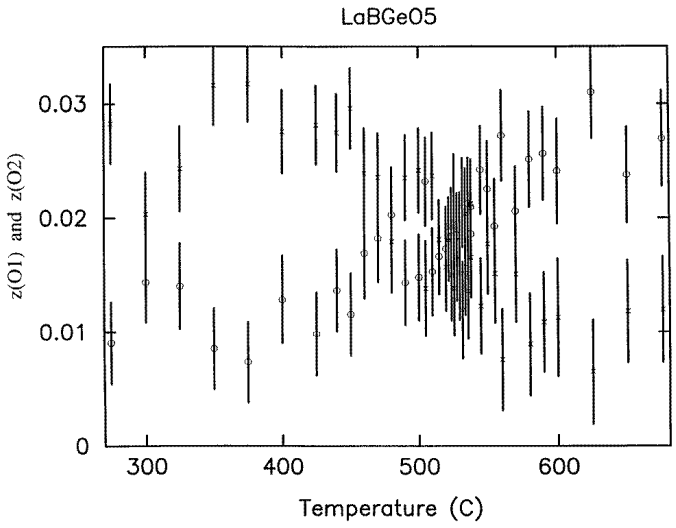


(c)

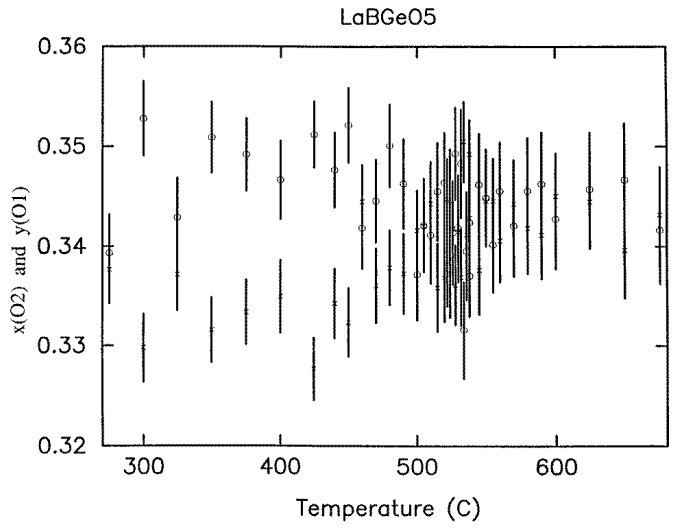


(d)

**Figure 4.** (Continued)

the data from the long runs at 535, 560 and 630 °C resulted in large values of $B_{22}$ and $B_{33}$ for the O5 ion and it became clear that it was necessary to modify the model by splitting the O5 position into two.

Profile refinements of the full sequence of short runs taken at some forty temperatures in the interval 275–675 °C allowed us to follow the evolution of the positional parameters of all of the atoms and to reach some conclusions about the atomic mechanism of the phase transition. To facilitate comparison, the low-temperature atomic coordinates were recalculated in the high-temperature setting, where the $a$-axis must be one of the twofold axes at $z = 1/3$ or 5/6 in the space group $P3_121$. Then the refinements of the short runs

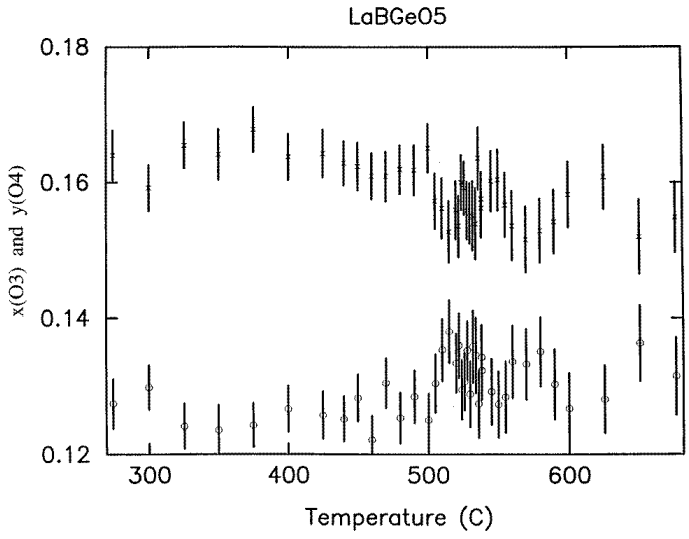


(e)

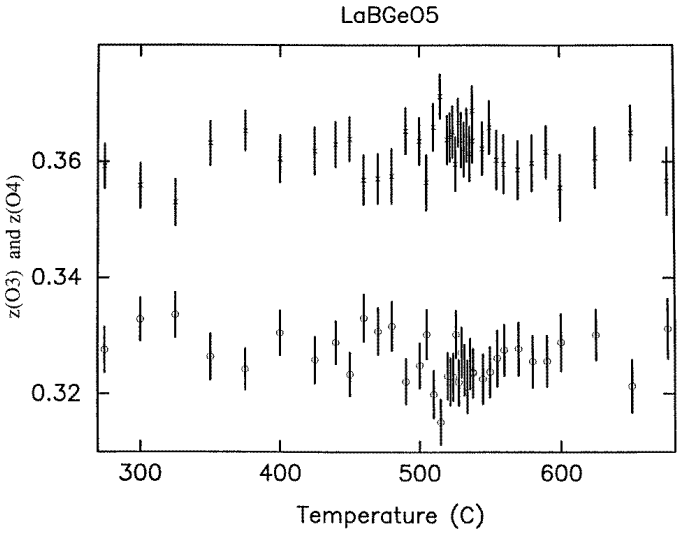


(f)

**Figure 4.** (Continued)

were carried out in the same space group $P3_1$ for both modifications throughout the whole temperature interval. In this way the results have not been influenced by imposing the non-polar space group above $T_c$. A large change occurs in the O5 $z$-parameter (figure 4(a)) which increases from $z = -0.22$ to $z = -0.18$ with a small change of slope at $T_c$ (see table 2). The O5 $x$- and $y$-parameters decrease (figure 4(b)) but the magnitudes of these changes are less than the change in the O5 $z$-coordinate. The final position of O5 does not lie on the twofold axis, but it is closer to it than in the low-temperature phase: more precisely, the O5 ion moves to a position halfway between that occupied at room temperature and the model position on the twofold axis (figure 3). A calculation of the maximally probable position

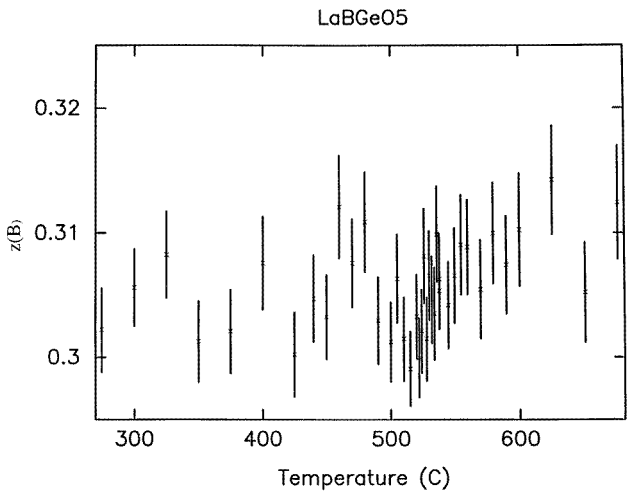


**Figure 4.** (Continued)

**Table 2.** The characteristics of the refinements of data from the long runs at elevated temperatures and the shorter run at ambient temperature (20 °C).

| $T$ (°C) | $R_p$ | $wR_p$ | $R_{exp}$ | $N-P+C$ | Basic variables | $\chi^2$ |
|---|---|---|---|---|---|---|
| 20 | 5.06 | 5.73 | 5.31 | 5749 | 37 | 1.17 |
| 500 | 2.46 | 2.94 | 1.96 | 5749 | 31 | 2.26 |
| 525 | 2.66 | 3.27 | 1.90 | 5749 | 39 | 2.96 |
| 535 | 2.27 | 2.71 | 1.77 | 5724 | 25 | 2.37 |
| 560 | 2.28 | 2.77 | 1.64 | 5749 | 25 | 2.85 |
| 630 | 2.24 | 2.68 | 1.53 | 3832 | 27 | 3.05 |

inside the vibration ellipsoid with large $B_{22}$- and $B_{33}$-parameters gave parameter values close to those derived from the thermal evolution study: $x \cong -0.0080$, $y \cong 0.0332$, $z \cong 0.8077$, assuming a split site with 50% occupancy.

Extending the thermal evolution analysis to the remaining atoms in the structure also provides further insight into the atomic mechanisms of the phase change. For example, the behaviour of the $z$-parameters of O1 and O2, which change in an opposite sense (figure 4(c)), means that not only does the internal edge O5–O5′ of the B tetrahedron move in the temperature interval 320–480 °C, but also so does the external edge O1–O2. The equality of the $z$-parameters at 530 °C means that, during the rotation of the B tetrahedron around the $3_1$ axis, the latter edge is horizontal (perpendicular to $\boldsymbol{c}$) at $T_c$ and then changes its slope at higher temperatures. Some changes appear in the O1 $y$- and O2 $x$-parameters (figure 4(d)) until maximal symmetry is reached when their values are equal. Since the positional parameters of the O3 and O4 atoms show little change (figures 4(e), 4(f)), we may conclude that the Ge–O tetrahedron is a much more stable unit during the phase transition than is the B–O tetrahedron. The $z$-parameter of the B atom increases slightly with temperature, but does not reach the exact value of 1/3 to lie on the twofold axis (figure 4(g)).

After the analysis of the thermal evolution of the structure using data from the short runs, we carried out accurate refinements of the low-temperature structure in the space group

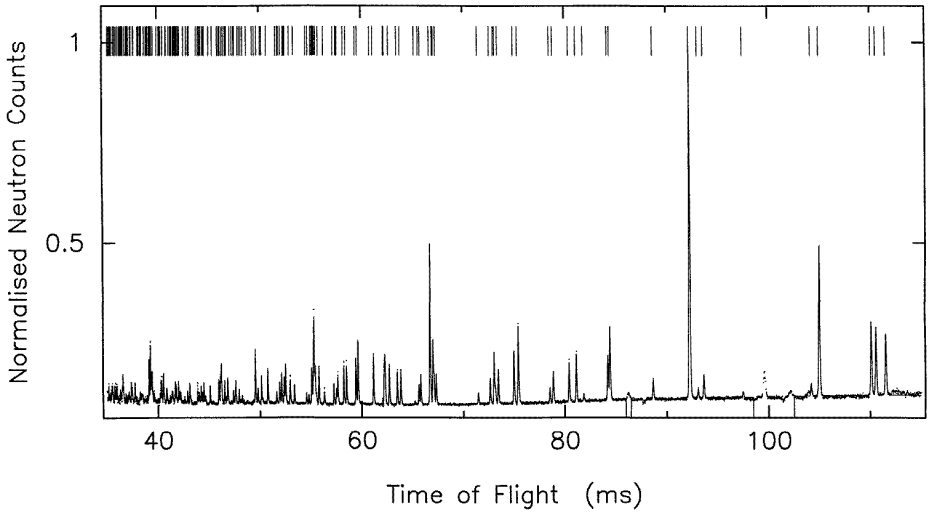


(a)

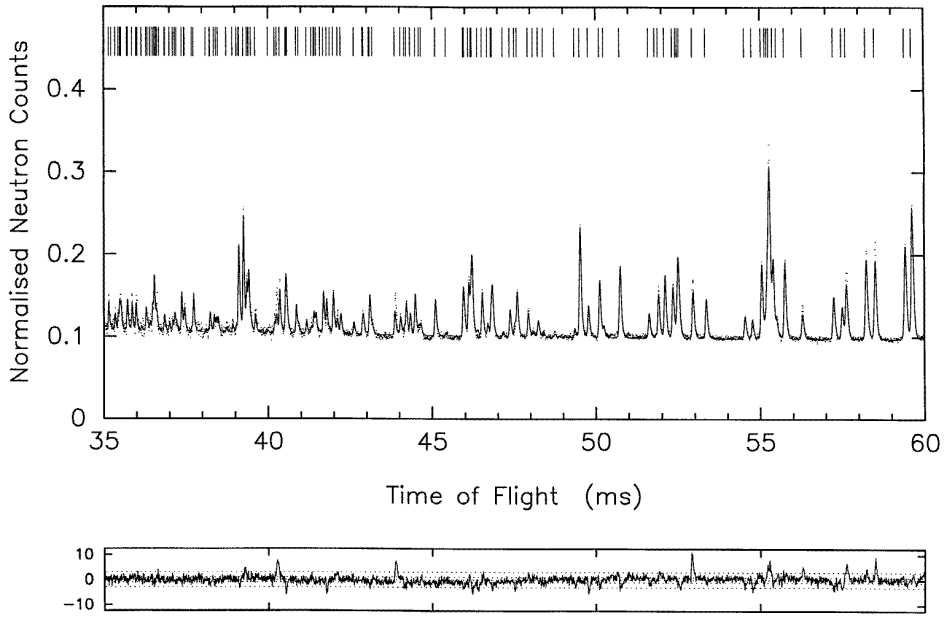


(b)

**Figure 5.** Powder profile refinements of $LaBGeO_5$. (a) and (b) show the low-temperature phase, using data taken at 525 °C, and (c) and (d) the high-temperature phase, using data taken at 535 °C; the patterns between 86.0 and 86.5 ms and between 98.5 and 102.5 ms have been excluded from the refinements since they contain features arising from an unidentified impurity. In (b) and (d) a part of the time-of-flight pattern is shown on a larger scale so that the fit at smaller *d*-spacings can be more easily appreciated. The difference between observed and calculated profiles divided by the estimated standard deviation (esd) of the observed profile is plotted in the lower pattern of each figure; horizontal dotted lines are drawn at ±1 and ±3 esd.

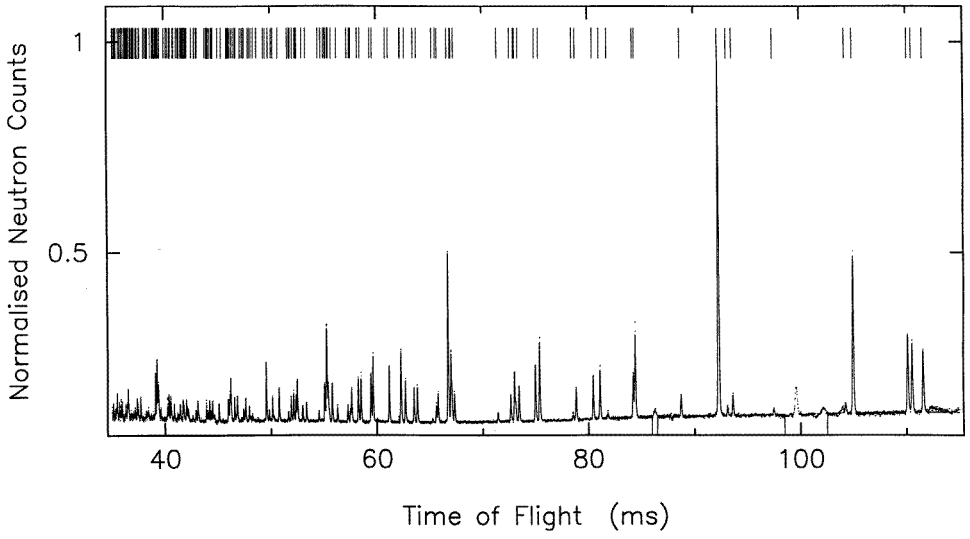


(c)

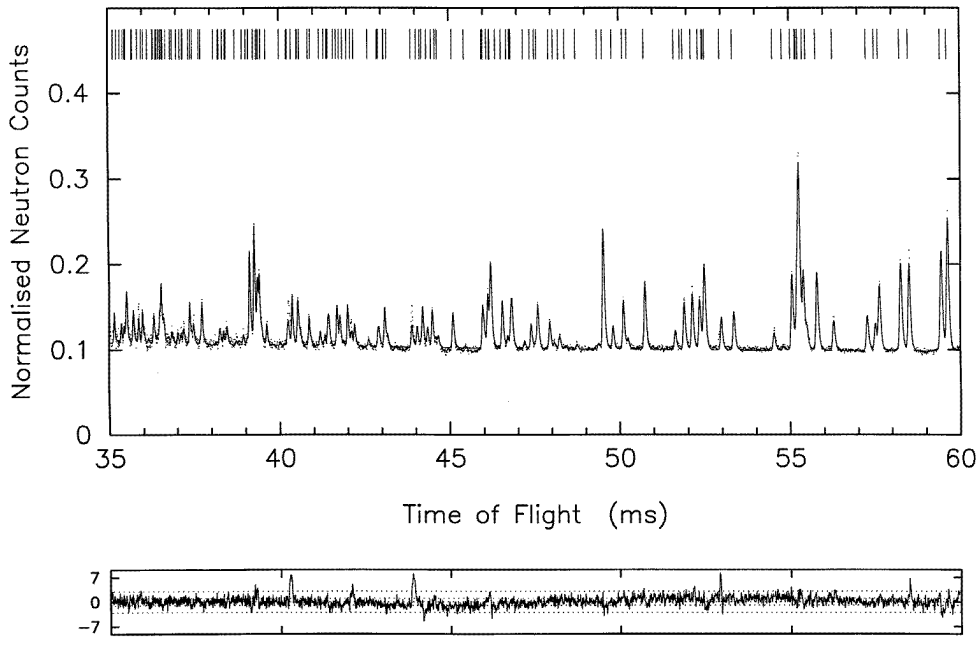


(d)

**Figure 5.** (Continued)

$P3_1$ using data from the long runs collected at three temperatures below $T_c$, including the shorter run at 20 °C for comparison with the x-ray study. The complexity of the model and the effects of the high degree of pseudosymmetry were reduced by using isotropic thermal vibration parameters for all atoms and constraining those parameters for the oxygen atoms to be equal.

**Table 3.** The positional and thermal parameters of the lower-temperature phase of $LaBGeO_5$ as determined at ambient temperature from x-ray single-crystal measurements [2], and at 20, 500 and 525 °C from neutron powder data in this study (the HT setting is used throughout).

| Atom | $T$ (°C) | $x/a$ | $y/b$ | $z/c$ | Site occupation | $B_{11}$ | $B_{22}$ | $B_{33}$ | $B_{12}$ | $B_{13}$ | $B_{23}$ |
|---|---|---|---|---|---|---|---|---|---|---|---|
| La | X-ray ambient | 0.4107(1) | −0.0007(1) | 1/3 | 1 | 0.37(1) | 0.28(1) | 0.37(1) | 0.14(1) | 0.00(1) | 0.03(1) |
| | 20 | 0.4107(8) | −0.0010(14) | 1/3 | 1 | 0.20(4) | | | | | |
| | 500 | 0.4072(5) | −0.0018(10) | 1/3 | 1 | 0.61(3) | | | | | |
| | 525 | 0.4078(6) | 0.0012(11) | 1/3 | 1 | 0.82(3) | | | | | |
| B | X-ray | −0.114(1) | −0.010(1) | 0.313(1) | 1 | 0.5(2) | 0.6(2) | 1.5(3) | 0.2(2) | 0.0(2) | −0.4(2) |
| | 20 | −0.1152(9) | −0.0122(15) | 0.3086(10) | 1 | 0.79(8) | | | | | |
| | 500 | −0.1059(7) | 0.0015(12) | 0.3175(8) | 1 | 1.50(5) | | | | | |
| | 525 | −0.1048(9) | 0.0029(17) | 0.3217(10) | 1 | 1.95(6) | | | | | |
| Ge | X-ray | 0.4200(3) | −0.0033(1) | 0.8345(4) | 1 | 0.25(2) | 0.38(2) | 0.20(1) | 0.20(1) | 0.00(3) | 0.01(3) |
| | 20 | 0.4180(7) | 0.0004(13) | 0.8433(11) | 1 | 0.17(4) | | | | | |
| | 500 | 0.4183(6) | −0.0013(9) | 0.8369(11) | 1 | 0.68(3) | | | | | |
| | 525 | 0.4201(6) | 0.0008(11) | 0.8317(13) | 1 | 0.90(4) | | | | | |
| O1 | X-ray | 0.1538(8) | 0.3438(8) | 0.0116(7) | 1 | 0.6(2) | 0.4(1) | 0.5(1) | 0.2(1) | 0.1(1) | −0.2(1) |
| | 20 | 0.1528(15) | 0.3428(16) | 0.0179(11) | 1 | 0.40(3) | | | | | |
| | 500 | 0.1543(10) | 0.3485(10) | 0.0201(9) | 1 | 1.08(3) | | | | | |
| | 525 | 0.1519(11) | 0.3506(14) | 0.0210(10) | 1 | 1.32(3) | | | | | |
| O2 | X-ray | 0.3320(9) | 0.1450(8) | 0.9912(8) | 1 | 0.4(1) | 0.6(2) | 0.9(2) | 0.2(1) | 0.1(1) | −0.2(1) |
| | 20 | 0.3356(15) | 0.1481(15) | −0.0011(12) | 1 | 0.40(3) | | | | | |
| | 500 | 0.3350(10) | 0.1494(10) | −0.0072(10) | 1 | 1.08(3) | | | | | |
| | 525 | 0.3344(12) | 0.1532(12) | −0.0071(11) | 1 | 1.32(3) | | | | | |
| O3 | X-ray | 0.1440(9) | 0.6125(8) | 0.3409(7) | 1 | 0.4(1) | 1.4(2) | 0.5(1) | 0.3(1) | −0.2(1) | −0.0(1) |
| | 20 | 0.1342(11) | 0.6089(13) | 0.3376(11) | 1 | 0.40(3) | | | | | |
| | 500 | 0.1268(8) | 0.6115(9) | 0.3360(8) | 1 | 1.08(3) | | | | | |
| | 525 | 0.1265(9) | 0.6120(10) | 0.3374(10) | 1 | 1.32(3) | | | | | |
| O4 | X-ray | 0.6101(8) | 0.153(1) | −0.3441(8) | 1 | 1.6(2) | 0.4(1) | 0.6(2) | 0.4(1) | 0.2(1) | 0.2(1) |
| | 20 | 0.6081(11) | 0.1620(11) | −0.3385(11) | 1 | 0.40(3) | | | | | |
| | 500 | 0.6066(8) | 0.1634(7) | −0.3402(10) | 1 | 1.08(3) | | | | | |
| | 525 | 0.6083(9) | 0.1632(8) | −0.3408(11) | 1 | 1.49(3) | | | | | |
| O5 | X-ray | 0.0131(9) | 0.057(1) | 0.7807(8) | 1 | 1.4(2) | 0.8(2) | 1.0(2) | 0.5(2) | −0.3(2) | −0.3(1) |
| | 20 | 0.0120(9) | 0.0542(7) | 0.7861(11) | 1 | 0.40(3) | | | | | |
| | 500 | −0.0123(6) | 0.0395(5) | 0.7959(9) | 1 | 1.08(3) | | | | | |
| | 525 | −0.0039(7) | 0.0367(6) | 0.7978(10) | 1 | 1.49(3) | | | | | |

## 5. The structure of the high-temperature phase of $LaBGeO_5$

Data from the three long runs above $T_c$ at 535, 560 and 630 °C were refined in the space group $P3_121$ to quantify the site splitting in the new model for the high-temperature phase. The higher symmetry of this phase allowed us to refine the oxygen thermal parameters

independently of each other. However, refinements made with the B atom on the twofold axis resulted in this atom having enlarged anisotropic temperature parameters $B_{ij}$ (mainly $B_{33}$), which clearly showed that the B position should be split, like that of the O5 atom, but in this case mainly in the ***c***-direction. In the final refinement, slack constraints were applied to the equality of the B–O(1) and B–O(1′) and of the B–O(5) and B–O(5′) interatomic distances to avoid the positional instability of the B atom due to its proximity to the twofold axis.

**Table 4.** The position and thermal parameters of the high-temperature phase of $LaBGeO_5$ at 535, 560 and 630 °C.

| Atom | *T* (°C) | *x* | *y* | *z* | Site occupation | $B_{11}$ | $B_{22}$ | $B_{33}$ | $B_{12}$ | $B_{13}$ | $B_{23}$ |
|---|---|---|---|---|---|---|---|---|---|---|---|
| La | 535 | 0.4076(3) | 0 | 1/3 | 1 | 0.78(3) | | | | | |
| | 560 | 0.4074(3) | 0 | 1/3 | 1 | 0.87(3) | | | | | |
| | 630 | 0.4071(4) | 0 | 1/3 | 1 | 0.93(3) | | | | | |
| B | 535 | −0.1079(4) | −0.0012(4) | 0.3225(8) | 0.5 | 1.77(5) | | | | | |
| | 560 | −0.1117(9) | −0.0085(18) | 0.3179(13) | 0.5 | 1.87(7) | | | | | |
| | 630 | −0.1112(9) | −0.0077(33) | 0.3217(20) | 0.5 | 1.81(8) | | | | | |
| Ge | 535 | 0.4198(3) | 0 | 5/6 | 1 | 0.76(3) | | | | | |
| | 560 | 0.4199(2) | 0 | 5/6 | 1 | 0.78(5) | | | | | |
| | 630 | 0.4197(5) | 0 | 5/6 | 1 | 0.69(6) | | | | | |
| O1 | 535 | 0.1516(3) | 0.3418(3) | 0.0157(3) | 1 | 0.88(4) | | | | | |
| | 560 | 0.1519(3) | 0.3423(3) | 0.0155(3) | 1 | 0.93(4) | | | | | |
| | 630 | 0.1521(4) | 0.3422(3) | 0.0163(4) | 1 | 1.04(5) | | | | | |
| O3 | 535 | 0.1444(3) | 0.6104(3) | 0.3392(3) | 1 | 2.12(9) | 0.66(6) | 1.95(7) | −0.43(8) | −0.35(8) | −0.24(6) |
| | 560 | 0.1440(3) | 0.6109(3) | 0.3389(4) | 1 | 2.16(9) | 0.71(7) | 2.07(7) | −0.40(8) | −0.47(8) | −0.27(7) |
| | 630 | 0.1441(4) | 0.6104(4) | 0.3391(4) | 1 | 2.3(1) | 0.66(8) | 2.26(9) | −0.34(9) | −0.46(9) | −0.27(9) |
| O5 | 535 | −0.0045(5) | 0.0366(5) | 0.8030(5) | 0.5 | 0.72(6) | | | | | |
| | 560 | −0.0052(5) | 0.0360(6) | 0.8047(5) | 0.5 | 0.78(6) | | | | | |
| | 630 | −0.0067(6) | 0.0344(8) | 0.8075(7) | 0.5 | 0.83(8) | | | | | |

The quality of fit obtained in the refinements of data from the long runs is summarized in table 2. Four final observed, calculated and difference plots of the diffraction patterns at 525 and 535 °C are presented in figure 5. The refined positional and thermal vibration parameters at the six temperatures are given in the same (HT) setting to facilitate intercomparison: the low-temperature structure in table 3, which also includes the results from the x-ray study, and the HT phase in table 4.

The splitting of the B position is less pronounced than that for the O5 position, and for both atoms decreases with increasing temperature. Thus the O5–O5′ distance varies from 0.61 Å at 535 °C through 0.59 Å at 560 to 0.55 Å at 630 °C. The interatomic distance between the two half-occupied positions B and B′ is much smaller: 0.17 Å at 535 °C, 0.15 Å at 560 °C and only 0.12 Å at 630 °C. The bridging O1 atom between B and Ge tetrahedra (figure 1) is hardly displaced over the whole temperature range and is characterized by a normal isotropic thermal vibration parameter. In contrast, the non-bridging O3 atom demonstrates a tendency towards splitting, as indicated by the enlarged $B_{11}$- and $B_{33}$-values (table 4) and the unequal *x* (O3) and *y* (O4) parameters, which are, however, still not sufficiently large to be split in our calculations. Finally, it should be noted that the thermal parameters of all of the atoms in the final structural model are of reasonable magnitude (table 4). It is recognized that Bragg diffraction data cannot distinguish between a 'split-atom' static model with a random distribution of atoms between two fixed sites and

a dynamic model in which the atom vibrates about one mean position. On the basis of several recent studies it is concluded [10] that, if the degree of disordering in a crystal leads to a significant contribution to the Debye–Waller factor, then the averaged mean square displacement must be presented as $u_\mu^2 = (u_\mu)_{stat}^2 + (u_\mu)_{dyn}^2$, where only the dynamic part is temperature dependent. We conclude that the temperature dependence of the distances between the split positions of O5–O5′ and B–B′ is evidence for the dynamic nature of the disordering in our case, but we intend to investigate this difficult question further using spectroscopic techniques.

## 6. Discussion

The structures of both the low- and high-temperature modifications of $LaBGeO_5$ have the same main features. They may be described as being built from chains of B–O and Ge–O coordination tetrahedra which are connected through the large La polyhedra (figure 1). The complicated B–Ge structural unit, which we describe as a chain, has a helical chain of B tetrahedra as a core, decorated with Ge tetrahedra outside, which are themselves connected through corner sharing with B tetrahedra at different heights (figure 6(a)).

**Table 5.** The temperature variation of cation–oxygen interatomic distances in the La polyhedron and the B and Ge tetrahedra.

| $T$ (°C) | La polyhedron (Å) | B tetrahedron (Å) | Ge tetrahedron (Å) |
|---|---|---|---|
| 20 | O1: 2.639; O1′: 2.768 | O1: 1.506 | O1: 1.776 |
| | O2: 2.685; O2′: 2.695 | O2: 1.513 | O2: 1.777 |
| | O3: 2.431; O3′: 2.566 | O5: 1.445 | O3: 1.626 |
| | O4: 2.590; O4′: 2.411 | O5′: 1.480 | O4: 1.764 |
| | O5: 2.672 | | |
| 500 | O1: 2.689; O1′: 2.811 | O1: 1.466 | O1: 1.782 |
| | O2: 2.702; O2′: 2.684 | O2: 1.564 | O2: 1.739 |
| | O3: 2.423; O3′: 2.622 | O5: 1.463 | O3: 1.688 |
| | O4: 2.580; O4′: 2.425 | O5′: 1.430 | O4: 1.697 |
| | O5: 2.726 | | |
| 525 | O1: 2.665; O1′: 2.808 | O1: 1.445 | O1: 1.799 |
| | O2: 2.712; O2′: 2.710 | O2: 1.573 | O2: 1.731 |
| | O3: 2.411; O3′: 2.622 | O5: 1.478 | O3: 1.710 |
| | O4: 2.589; O4′: 2.427 | O5′: 1.422 | O4: 1.675 |
| | O5: 2.740 | | |
| 535 | O3(×2): 2.408 | O1: 1.516 | O1(×2): 1.760 |
| | O3′(×2): 2.598 | O1′: 1.516 | O3(×2): 1.697 |
| | O1(×2): 2.680 | O5: 1.451 | |
| | O1′(×2): 2.771 | O5′: 1.451 | |
| | O5(×2): 2.747 | | |
| 560 | O3(×2): 2.406 | O1: 1.517 | O1(×2): 1.760 |
| | O3′(×2): 2.603 | O1′: 1.517 | O3(×2): 1.697 |
| | O1(×2): 2.679 | O5: 1.453 | |
| | O1′(×2): 2.770 | O5′: 1.453 | |
| | O5(×2): 2.750 | | |
| 630 | O3(×2): 2.408 | O1: 1.516 | O1(×2): 1.760 |
| | O3′(×2): 2.604 | O1′: 1.516 | O3(×2): 1.696 |
| | O1(×2): 2.681 | O5: 1.454 | |
| | O1′(×2): 2.778 | O5′: 1.454 | |
| | O5(×2): 2.762 | | |

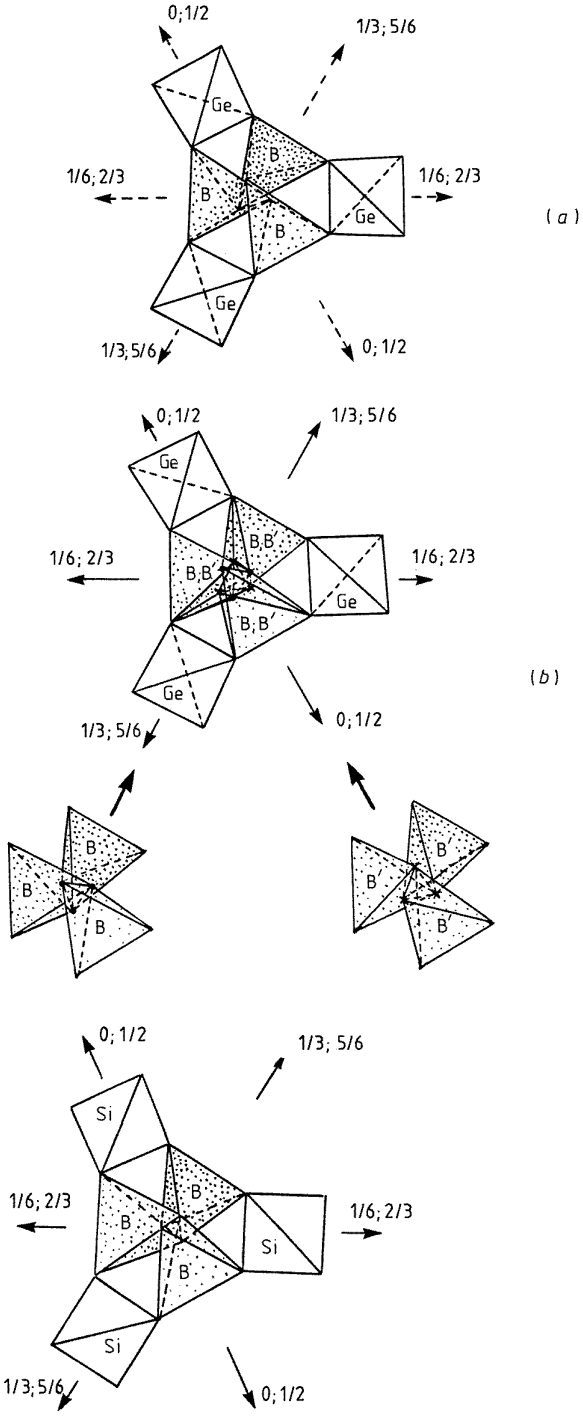


**Figure 6.** The structural fragment in three different variants of the stillwellite structure type projected down [001] showing the helical chains of tetrahedra. (a) The low-temperature modification of $LaBGeO_5$, (b) the high-temperature phase of $LaBGeO_5$ with double helical chains of tetrahedra, including separately two neighbouring helical chains, and (c) the high-temperature modification of $LaBSiO_5$.

The splitting of the positions of O5 and B at temperatures above $T_c$ into two sites with equal (50%) occupation produces the crystal chemical result that the helical chain of B–O tetrahedra around the $3_1$ axis is doubled by the twofold axis: the resulting dynamically disordered double helix has no polarity in the ***c***-direction (figure 6(b)). This is the main reason for the ferroelectric properties disappearing at $T_c$, and the phase is paraelectric at temperatures above 530 °C.

The B–O and Ge–O tetrahedra have interatomic distances (table 5) within the normal range of values, for example: B–O, 1.516–1.454 Å at 630 °C; and Ge–O, 1.760–1.696 Å. The interatomic distance between B and O5 must be chosen from both, B and O5, of one orientation of the helix or one correct couple between the four split positions.

The La-atom coordination increases from nine (LT) to ten (HT) because of the change in the position of O5. In reality, only one oxygen between two (O5 and O5′) split positions participates in the coordination of the La atom.

Specific heat measurements by Onodera *et al* [9] show that there is a small excess entropy, $\Delta S = 0.114R = R\ln(1.121)$, associated with the phase transition implying that the transition must be principally displacive in character. However, this small excess entropy is consistent with the disorder of one of the eight atoms in the formula unit.

The ionic radii of the rare-earth ions and of the Ge (or Si) ions in their oxygen tetrahedra play a very important role in this structure type. An analysis of the refined crystal structure of the silicon analogue $LaBSiO_5$ [11] shows that, even at room temperature where the polar modification is stable, the atomic arrangement is close to that of our first simple HT model. The $a/c$ ratio is 1.0096 in comparison to the value of 1.0206 for $LaBGeO_5$ at ambient temperature. The latter only becomes smaller at temperatures closer to $T_c$ (530 °C). The positions of the La, Si and B atoms in $LaBSiO_5$ are practically special (taking into account their standard deviations) and are located in the position corresponding to the twofold axes in the HT-modification; O1 is equivalent to O2 and O3 to O4; O5 is very close to the optimum position on the twofold axis at $z = 5/6$. Therefore in $LaBSiO_5$ smaller displacements are necessary in order to reach the paraelectric state, and its lower transition temperature ($T_c = 140$ °C) [12] can be easily understood from the Abrahams, Jamieson, Kurtz criteria [13]. Recently, an x-ray single-crystal study of $LaBSiO_5$ [14] has confirmed that the paraelectric phase has a structure which corresponds to our simple model without the splitting of the O5 site (figure 6(c)). The smaller size of the Si–O tetrahedra forces the B–O tetrahedra to rotate about the $3_1$ axis, and this may be compared to the effect of high pressure, and results in a tilting of the B chain. In the case of the larger Ge–O tetrahedron, the O5–O5′ edge of the B–O tetrahedron is more vertical and the chain looks less tilted (figure 6(a)). We may postulate the existence of a high-pressure modification of $LaBGeO_5$ equivalent to $LaBSiO_5$. The HT modification of $LaBGeO_5$ represents some intermediate case with partial rotation ($\sim 15°$) of O5 and the B–O tetrahedron around the $3_1$ axis and a doubling of the chain (figure 6(b)).

## Acknowledgments

We should like to thank Dr B V Mill' for preparing and giving us the single-crystal material for the investigation, Professor V G Tsirelson for helpful discussions and Drs C Wilkinson and G M McIntyre for measuring the wavelength dependence of our sample absorption. We are indebted to the referee whose expert and critical reading of our initial manuscript greatly improved the final version. We are grateful to the Royal Society for financial support for this work which forms part of the Society's Joint Research Project 638072 P/737 and to INTAS for their support under Project 1010-CT93-0061.

## References

[1] Voronkov A A and Pyatenko Yu A 1964 *Kristallografia* **12** 258
[2] Belokoneva E L, Mill' B V, Butashin A V and Kaminskii A A 1991 *Izv. Akad. Nauk SSSR, Ser. Neorg. Mater.* **27** 556
[3] Kaminskii A A, Mill' B V, Belokoneva E L and Butashin A V 1990 *Izv. Akad. Nauk SSSR, Ser. Neorg. Mater.* **26** 1105
[4] Kaminskii A A, Butashin A V, Maslyanizin J A, Mill B V, Mironov V S, Rozov S P, Sarkisov S E and Shigorin V C 1991 *Phys. Status Solidi* a **125** 671
[5] Horiuchi N, Osakabe E, Uesu Y and Strukov B A 1995 *Ferroelectrics* **169** 273
[6] Pisarev R V and Seran M 1995 *Fiz. Tverd. Tela* **37** 3669
[7] Stefanovich C Yu, Mill' B V and Butashin A V 1992 *Kristallografia* **37** 965
[8] Uesu Y, Horiuchi N, Osakabe E, Omori S and Strukov B A 1993 *J. Phys. Soc. Japan* **62** 2522
[9] Onodera A, Strukov B A, Belov A A, Taraskin S A, Haga H, Yamashita H and Uesu Y 1993 *J. Phys. Soc. Japan* **62** 4311
[10] Tsirelson V G 1993 Chemical bond and thermal motion of atoms in crystal *Itogi Nauk. Tekh., Ser. Kristallochim.* **27** 1–269 (in Russian)
[11] Samigina V R, Genkina E A, Maximov B A and Leonyuk N I 1993 *Kristallografia* **38** 61
[12] Stefanovich S Yu, Sigaev V N, Dechev A V, Mosunov A V, Samigina V R and Sarkisov P D 1995 *Izv. Ser. Neorg. Mater.* **31** N6
[13] Abrahams S C 1994 *Acta Crystallogr.* A **50** 658
[14] Belokoneva E L, Shuvaeva V A and Antipin M Yu 1995 *Zh. Neorg. Chim.* **41** 1097